Fabrication and characterization of improved Ag/PS hollow-glass waveguides for THz transmission

Carlos M. Bledt,[1,2,*] Jeffrey E. Melzer,[1] and James A. Harrington[1]

[1]School of Engineering, Rutgers University, 607 Taylor Road, Piscataway, New Jersey 08854, USA

[2]School of Engineering, Brown University, 182 Hope Street, Providence, Rhode Island 02912, USA

*Corresponding author: carlos_bledt@brown.edu

Received 3 June 2013; revised 12 August 2013; accepted 13 August 2013;
posted 19 August 2013 (Doc. ID 191591); published 13 September 2013

This study involves the fabrication and characterization of improved quality silver (Ag)/polystyrene (PS) thin-film-coated hollow-glass waveguides for the low-loss transmission of terahertz radiation via modified dynamic liquid phase deposition techniques. High-quality PS thin films were deposited from aqueous PS solutions, and the spectral response of fabricated samples was measured from $\lambda = 1$–100 μm. Fabricated samples exhibited highly defined spectral responses throughout this entire range indicative of PS films of excellent quality. The spectra of experimental samples were compared to the theoretical and bulk PS spectra in the near-IR and far-IR regions. The thickness of deposited PS thin films was found to depend on total sample length and to vary from approximately 10–16 μm for sample lengths ranging from 115 to 140 cm. Such PS film thicknesses are adequate for low-loss delivery from approximately 2–4 THz. Furthermore, film thickness was found to vary minimally along the waveguide length regardless of total sample length. © 2013 Optical Society of America

OCIS codes: (310.1860) Deposition and fabrication; (060.2390) Fiber optics, infrared; (300.6270) Spectroscopy, far infrared; (300.6495) Spectroscopy, terahertz; (310.2785) Guided wave applications; (310.6188) Spectral properties.

http://dx.doi.org/10.1364/AO.52.006703

1. Introduction

Recent and ongoing research involving the emission, detection, transmission, and manipulation of terahertz (THz) frequencies has led to increased interest in the development of THz devices. Novel applications involving THz waves continue to surface as innovations in THz frequency sources and detectors continue to be developed. As such, it is of interest to develop a reliable waveguide for the low-loss transmission of THz radiation. To date, several types of waveguides have been developed for transmitting THz waves. These waveguides include planar mirrors, solid metal wires, solid dielectric, and rectangular or circular metal hollow. Many of these waveguides have exhibited only limited functionality for optimal THz wave transmission as a result of high losses, low efficiency coupling, and undesirable dispersion effects [1–4]. Recently, improved metal-coated hollow waveguides (HWs) incorporating dielectric thin films for enhanced reflection have shown promise for use as low-loss THz waveguides. One such practical metal/dielectric coated waveguide design is the hollow glass waveguide (HGW), which has been widely used for applications involving low-loss broadband transmission at infrared (IR) wavelengths [5–10]. The basic structure of HGWs is shown in Fig. 1 and consists of a reflective-silver thin film deposited on the inner surface of fused silica tubing over which a thin dielectric film of an appropriate optical material is deposited. In practice, it is important to select a dielectric material that exhibits low absorption in the wavelength region of interest and can be deposited from solution to achieve a high-quality uniform film. Additionally, it is essential to

1559-128X/13/276703-07$15.00/0
© 2013 Optical Society of America

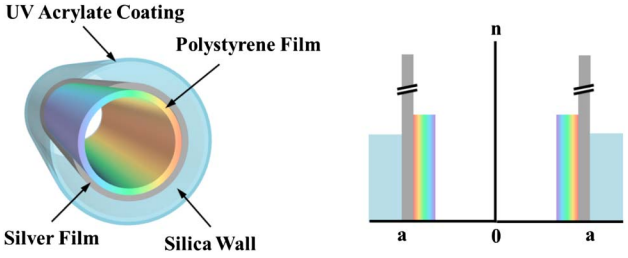

Fig. 1. Cross-sectional representation of metal/polystyrene-coated HGW.

design the waveguide based on the wavelength(s) of operation as the loss in HWs is fundamentally proportional to λ^2/a^3 where λ is the wavelength of light, and a is the bore radius of the silica capillary. This fundamental loss dependency of HWs is derived using the wave optics propagation loss analysis first established by Miyagi and co-workers [11,12].

2. Waveguide Optimization and Theory

In practice, potential candidates for use as dielectric thin film materials are limited in the THz regime. On one hand, the number of highly transparent materials in the THz and far-IR (FIR) regions is rather low, consisting mostly of polymers and specialized polymeric materials. Furthermore, optically suitable candidate THz transparent materials need to be deposited from a solution in order to be deposited as high-quality optical thin films in HGWs with the liquid phase deposition techniques used in this study. Particular candidates of interest include cyclic olefin polymers (COP), polymethylpentene (TPX), and polystyrene (PS) as these polymers can be deposited from solution and exhibit relatively low loss at THz frequencies [13]. In this study, PS was selected as the polymer of choice due to its low absorbance at THz frequencies, simultaneous low loss in the visible and near-IR (NIR) regions, and relative ease of deposition from solution [5–8,13]. To optimize design parameters, the optical response of Ag/PS coated HGWs at THz frequencies was calculated. Such theoretical analysis involved determining the attenuation coefficient as a function of HGW bore radius, wavelength, and PS film thickness at THz frequencies. The waveguide loss theory developed by Miyagi and Kawakami [12] is based on wave optics physics and has been widely used to accurately predict the minimal theoretical loss of HGWs. Using this method, the attenuation for the hybrid (HE) modes, which exhibit the lowest loss in metal/dielectric coated HGWs, may be calculated from [12]

$$\alpha = \left(\frac{u_{nm}}{2\pi}\right)^2 \frac{\lambda^2}{a^3}\left(\frac{n_m}{n_m^2+\kappa_m^2}\right)\left(\frac{1}{2}\left(1+\frac{n_F^2}{\sqrt{n_F^2-1}}\right)^2\right), \quad (1)$$

where u_{nm} is the mode parameter, λ is the wavelength, a is the HW bore radius, n_m is the real part of the refractive index of the metal, κ_m is the imaginary part of the refractive index of the metal, and n_F is the real part of the refractive index of the dielectric. For calculations, the refractive index for Ag used was $305–i529$ ($\lambda \approx 100–110$ μm), and PS was assumed to be a lossless dielectric with a constant refractive index of $n = 1.58$ in this frequency range [13,14]. The optimal PS film thickness necessary to achieve the lowest loss for HE modes at the design wavelength is given by [11,12]

$$d_o = \frac{\lambda_d}{2\pi\sqrt{n_F^2-1}} \tan^{-1}\left(\frac{n_F}{(n_F^2-1)^{\frac{1}{4}}}\right), \quad (2)$$

where λ_d is the design wavelength, and n_F is the real part of the refractive index of PS at λ_d. Using Eq. (2), the optimal dielectric thin film thickness for PS at THz frequencies was calculated and is given in Fig 2. PS films of optimal thicknesses for the transmission of THz waves in this range may in fact be achievable in practice using fabrication methods based on current procedures used for fabricating Ag/AgI, Ag/CdS, and Ag/PbS HGWs for use at IR wavelengths [5–7,11,15]. For this particular study, the target frequency range was selected to be $\nu = 2.50–3.75$ THz ($\lambda = 80–120$ μm), corresponding to an optimal PS film thickness of $d_o = 10.0–15.0$ μm. For a given propagating wavelength, loss increases with decreasing bore size as the number of propagating modes decreases, thus presenting a trade-off between output mode quality and total throughput power, requiring the waveguide parameters to be adequately selected for the desired application and required response. Experimentally, it has been shown that metal/dielectric coated HWs can be considered largely single mode when the inner diameter is equal to or less than approximately 30λ. Thus, for the waveguides fabricated in this study with ID $= 2a = 1000$ μm, the single-mode behavior can be assumed at wavelengths greater than approximately $\lambda = 30–35$ μm [15].

In HGW design and fabrication parameter selection, it is often highly desirable to theoretically determine the expected spectral response in the wavelength region(s) of interest. Often, it is desirable to determine the expected spectral response for the particular dielectric thin film structure, particularly

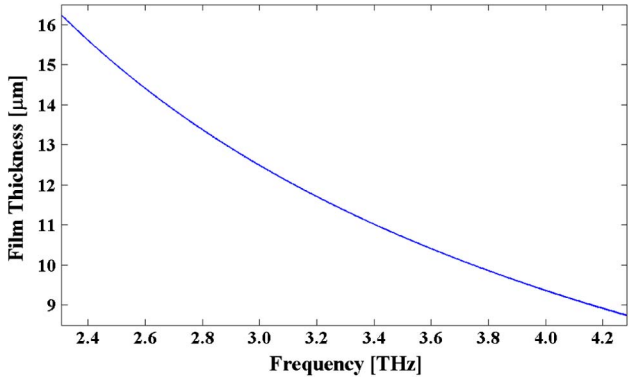

Fig. 2. Optimal PS film thickness as a function of frequency.

as a function of the deposited dielectric thin film thickness. Theoretical calculation of the spectral response is most conveniently performed via ray optics analysis. For a straight HW, the attenuation as a function of surface reflectance, R, bore size, a, and propagation angle, φ, is given by [11,16–18]

$$\alpha = \frac{1 - R}{4a \cot \varphi}, \tag{3}$$

where the surface reflectance in turn depends on the wavelength of light, polarization, incident angle ($\theta = 90 - \varphi$), and surface thin film structure (including refractive index and film thickness). Several methods may be employed to determine the reflection coefficient with one of the most versatile, the ray transfer matrix method, which is used in this study. The theoretical spectra presented throughout this study were derived using an iterative algorithm in which the reflection coefficient was calculated at discrete wavelength intervals within the desired spectral range to determine the propagation loss using Eq. (3). For all calculated spectra, propagation angles between $\varphi = 0.1$–$3.0°$ were used, as such propagation angles correspond to successfully propagating rays in HGWs of this bore size.

3. Fabrication Method

Experimental samples fabricated in this study consisted of 1000 μm ID by 1600 μm OD circular fused silica capillaries fabricated by Polymicro Technologies, Inc. All Ag/PS HGWs were prepared by first depositing a high-quality reflective silver thin film on the inner surface of the glass capillaries using a dynamic liquid phase deposition (DLPD) technique developed in part as a standard for fabricating HGWs for use at IR wavelengths [11]. The silver thin film deposition procedure was carried out using a peristaltic pump to obtain a steady fluid speed through the HW of approximately 70 cm/s at a plating solution temperature of 20°C. In practice, an Ag deposition time of 15 min was used. The Ag film thickness was larger than 0.6 μm, which is much greater than the penetration depth at THz frequencies.

A dielectric PS thin film was then deposited on the Ag-coated HGWs using a slightly modified DLPD procedure. Given that the DLPD process relies on aqueous precursor solutions, the first step was to prepare PS solutions of varying concentrations by dissolving PS pellets in toluene. This method has been successfully used in past work to prepare PS solutions up to 25 wt. % [5–7], although in this study only 15 wt. % PS solutions are used. The deposition of PS films is based on physical parameters such as viscosity, which increases with PS solution concentration and cohesive and adhesive forces. In practice it is necessary to achieve good film thickness uniformity to fabricate low-loss waveguides. In some previous studies, the Ag/PS HGWs were made using the peristaltic pump to push the solution through the silica tubing. This led to less uniform PS films as a result of the pulsating nature of the pump. To make more uniform films, the fabrication approach was modified, and a vacuum pump was used to pull the solution rather than using a peristaltic pump to push the solution through the tubing [5–7,11].

Successive samples fabricated using a vacuum pump showed a high degree of uniformity and consistency in the flow of the PS solution, although there was generally less control of the solution speed. To better control the PS solution speed, a flow meter was incorporated prior to the vacuum pump to reduce the effective pull of the vacuum pump. In addition, a closed system trap was introduced to collect PS solution waste. The modified DLPD system for the improved deposition of PS thin films is shown in Fig. 3. Using this modified DLPD method, PS films were successfully deposited in Ag-coated HGWs up to 140 cm in length.

All PS coatings were deposited keeping the volume of PS solution used consistent at $V = 2$ mL regardless of sample length. It was found that by decreasing the sample length, thicker films could be obtained. As the PS solution volume used was held constant regardless of waveguide length, it is logical that flowing the same quantity of solution along a longer waveguide would result in the deposition of a thinner PS film. It also was found that using solution concentrations less than 15 wt. % PS also did result in thinner high-quality, uniform films, while using either solution concentrations greater than 15 wt. % PS or using a flow speed in excess of 30 cm/min resulted in low-quality PS films. As the focus of this particular study was to fabricate Ag/PS HGWs for use at THz frequencies, thick PS films were necessary, and therefore a 15 wt. % PS solution concentration was used. All PS-coated samples were allowed to dry for at least 24 h using pressurized dry air at a flow rate of approximately 200 mL/min. Samples for determining the quality of fabrication method were either 115 or 140 cm in length.

4. Infrared Measurements

Optical characterization of Ag/PS HGW samples involved measuring the IR spectral response ranging

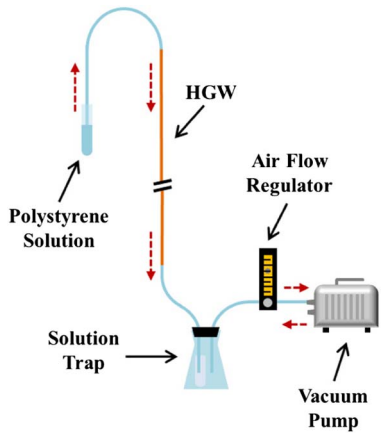

Fig. 3. Schematic of modified DLPD configuration for deposition of PS dielectric thin films.

from $\lambda = 1$–100 μm. The spectra of the Ag/PS samples was obtained using Fourier-transform infrared (FTIR) spectroscopy employing a range of light sources, instrument optics, and detectors, depending on the spectral region being investigated. Experimentally obtained spectral responses for the samples produced in this study were used for qualitative and quantitative analysis of deposited PS thin films; in particular to determine PS film quality, uniformity, and thickness. Furthermore, the experimental spectra were compared to simulated spectra for HGWs of appropriate PS thin film thicknesses as well as the spectral response of polystyrene itself. The PS refractive index used in all calculations was taken to be $n = 1.58$, which is appropriate given the minimal dispersion of PS in this wavelength range [13].

A. Near-Infrared Measurements and Film Thickness Calculations

NIR characterization involved measuring the spectral response from $\lambda = 1$–5 μm. In this region, PS is highly transparent, largely free of inherent spectral features, and its refractive index is nearly constant and approximately equal to that at THz frequencies; that is, $n = 1.58$. NIR spectral measurements were made using a Bruker Tensor 37 FTIR and a cryogenic InSb detector. Light from a broadband white-light source was coupled into 10 cm waveguide sample segments via a right-angle silver-coated off-axis parabolic mirror, and the output signal was collected by the cryogenic detector. A typical NIR spectral response for the Ag/PS HGWs is shown in Fig. 4. As seen from Fig. 4, the NIR spectral response obtained for these samples exhibited excellent film quality, uniformity, and thickness relative to the HGWs fabricated previously. The characteristic PS hydrocarbon absorption bands from approximately $\lambda = 3.4$–3.7 μm and $\lambda \sim 4.45$ μm are clearly visible along with sharp interference fringes due to the PS thin film throughout the entire wavelength range. Furthermore, this method for depositing PS thin films could be reproduced with much greater consistency than previous work on the same structures. The highly superior quality of the spectral response within this region relative to those obtained in previous studies for which a peristaltic pump was used [5,6] confirm the successful deposition of improved optical PS thin films in HGWs using the present method.

In addition to providing qualitative analysis for confirming the successful deposition of a high-quality PS films, the NIR spectral response was used to quantitatively approximate the thickness of the films by taking an average of the distance in wave numbers between subsequent interference fringes as determined from Eq. (4) [5–7,11,12]:

$$d = \frac{\left(\frac{1}{N}\sum_{i=2}^{N} \tilde{v}_N - \tilde{v}_{N-1}\right)^{-1}}{4\sqrt{n_F^2 - 1}}, \tag{4}$$

where N is the total number of fringes used for the calculation, $\tilde{v}$ is the centroid spectral wave number location of the Nth interference fringe, and n_F is the real part of the refractive index of PS at the wavelength region in question. Since Eq. (4) relies on the relative difference between interference fringes, the order of the interference fringes need not be explicitly known. Figure 5 shows an optimal spectral response using this method for determining PS dielectric thin film thickness from the location of successive interference fringes in the NIR region of the spectrum. The region between $\lambda = 1.21$–2.11 μm in the Ag/PS HGW experimental spectral response given in Fig. 5 has been converted to its respective wave number scale and plotted along with the calculated spectral response of a PS thin film of thickness equal to that calculated for this sample of 10.3 μm. To confirm this calculated thin film thickness, the theoretical spectral response for an Ag/PS-coated HGW with a PS thin film thickness input of 10.3 μm was obtained and compared to the experimentally obtained spectrum. The experimental response is seen to closely match the theoretical spectrum in this region, with the appearance of characteristic narrow, wave-number-dependent periodic interference fringes of alternating low and high intensities. Such clean

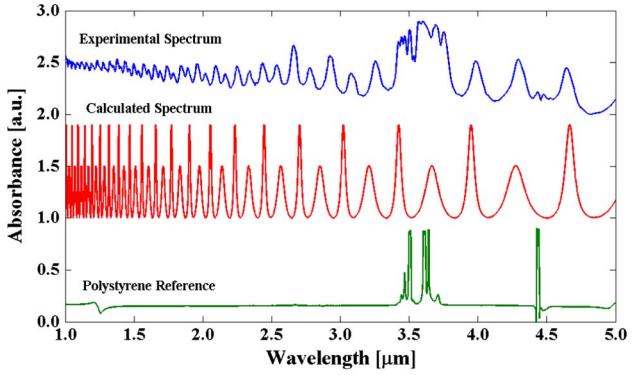

Fig. 4. Experimental NIR spectral response of Ag/PS HW having a dielectric PS film thickness of 10.3 μm along with corresponding simulated spectrum and PS thin-film reference.

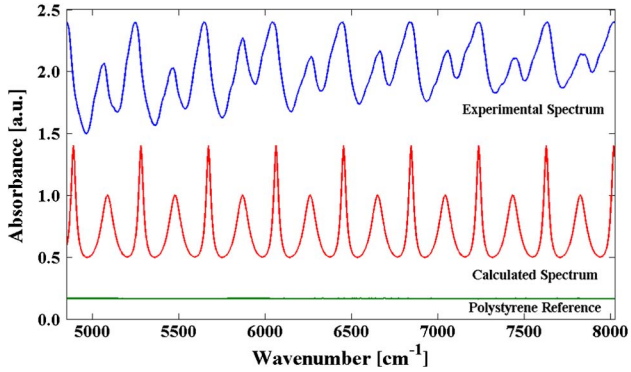

Fig. 5. Comparison of experimental and calculated spectral response as a function of wavenumber in the NIR region showing interference fringes used for determining PS film thickness.

interference spectra permit an accurate determination of film thickness. As previously mentioned, this specific wavelength region is selected for film-thickness analysis due to the combined transparency and the largely featureless spectral response of PS. It furthermore should be noted that the increasing absorbance with increasing wave number (or inversely with decreasing wavelength) is due to the combined effects of surface-roughness related scattering losses and increasing loss due to the underlying silver film. While seemingly contradictory to the fundamental λ^2 loss dependency of HGWs, this increasing absorbance seen at these shorter wavelengths is not a fundamental loss mechanism of HWs, but rather of the increased surface-roughness-related scattering, which becomes more pronounced at shorter wavelengths, and the increasing absorption coefficient of silver toward the visible region. In practice, all of these loss mechanisms contribute to the overall HW absorbance as a function of wavelength.

B. Mid- and Far-Infrared Measurements

Mid-IR (MIR) characterization involved measuring the spectral response from $\lambda = 5$–15 μm using a Bruker Tensor 37 FTIR with MIR optics and a MCT/A detector. In this region, PS exhibits much less transparency than in the NIR region with numerous spectral features and absorption peaks. It is therefore not a suitable region for precise qualitative or accurate film-thickness determination. Despite the inability to obtain extensive information in this spectral region, the MIR response of the 10.3 μm thick PS thin film sample shown in Fig. 6 was obtained for complete IR analysis and is presented along with the simulated and PS reference spectrum. As seen in Fig. 6, the inherent PS response has numerous absorption peaks and features in this region due to interatomic vibrations and characteristic molecular absorptions.

Final IR spectral response analysis involved FIR measurements from $\lambda = 20$–100 μm using a Bruker Tensor 37 FTIR with FIR optics and a DGTS detector. While not as optimal for film-thickness measurements, the inherent PS response is still featureless enough in the FIR that it can be used for important analysis. In particular, toward the far limit of this region ($\lambda > 45$), the inherent PS response is featureless enough and exhibits adequate transparency for detailed analysis. More importantly, it is for these high-THz frequencies that these Ag/PS HGWs are designed and optimized. Figure 7 presents the experimental FIR spectral response, along with the theoretical and PS reference responses for the 10.3 μm thick polystyrene Ag/PS HGW. From Fig. 7, it can be seen that this HGW exhibits a very clean spectral response in the FIR, with a primary interference peak at $\lambda = 49.6$ μm ($\nu \approx 6.04$ THz). Using a simplified version of Eq. (5), in which the only the centroid wavelength of the first interference peak is taken into account, the dielectric thin film thickness (in this case PS, $n = 1.58$), can be calculated directly as follows [11]:

$$d_F = \frac{\lambda_c}{4\sqrt{n_F^2 - 1}}, \tag{5}$$

where λ_c is the centroid wavelength of the first interference peak, and n_F is the real part of the refractive index of PS at the wavelength region in question. Using Eq. (5), the PS thin film thickness is determined to be approximately 10.2 μm, nearly equal to that obtained using successive absorption fringes in the NIR region using Eq. (4). After calculating the PS film thickness using Eq. (5), the corresponding optimal transmission wavelength can be determined using Eq. (6). For the samples fabricated in this study, it was found that the deposited PS film thicknesses of approximately 10.3 μm corresponded to optimal transmission at a wavelength of approximately $\lambda = 82.5$ μm ($\nu \approx 3.6$ THz) [11]:

$$\lambda_0 = 2\pi d_F \sqrt{n_F^2 - 1}\left[\tan^{-1}\left(\frac{n_F}{(n_F^2 - 1)^{\frac{1}{4}}}\right)\right]^{-1}, \tag{6}$$

where λ_c is the centroid wavelength of the first interference peak, and n_F is the real part of the refractive index of PS at the wavelength region in question. The experimental spectrum in Fig. 7 agrees with this

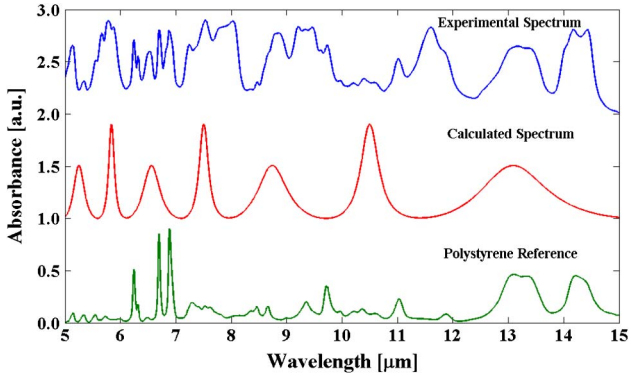

Fig. 6. Experimental MIR spectral response of Ag/PS HW having a dielectric PS film thickness of 10.3 μm along with corresponding simulated spectrum and PS thin-film reference.

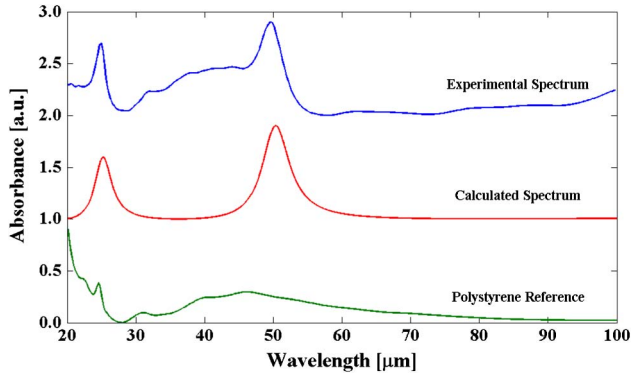

Fig. 7. Experimental FIR spectral response of Ag/PS HW having a dielectric PS film thickness of 10.3 μm along with corresponding simulated spectrum and PS thin-film reference.

calculation, with a minimal absorption region ranging from approximately $\lambda \approx 55$–76 μm ($\nu \approx 3.9$–5.5 THz), which is slightly shorter than the calculated optimal wavelength.

C. Polystyrene Film Thickness Dependency on HGW Length

All PS thin films deposited in this study were fabricated using a 15 wt. % PS solution. Samples having a total length of 140 cm had a mean PS film thickness of 10.25 μm ± 10%, corresponding to a minimal-loss wavelength of $\lambda \approx 82$ μm ($\nu \approx 3.66$ THz). Other samples were 115 cm in length. It was found from the IR spectra that these shorter-length samples had a mean PS film thickness of 15.9 μm ± 14%, corresponding to a minimal-loss wavelength of $\lambda \approx 127$ μm ($\nu \approx 2.36$ THz). Figure 8 gives the experimental spectral responses for 10 cm long segment obtained from fabricated samples initially at 115 and 140 cm in length for qualitative comparison. The PS film thickness for the 115 cm long sample was calculated to be 15.9 μm while, as previously discussed, that for the 140 cm long sample was found to be 10.3 μm. Furthermore, from Fig. 8, it can be seen that a clean spectral response is achieved despite increasing the fabricated waveguide length from 115 to 140 cm. The difference of PS film thickness for samples of different lengths demonstrate a dependence of deposited PS film thickness on total HGW length as we would expect based on our approach of using a fixed volume of PS to coat the guides.

Further PS film analysis involved determination of film variation along HGW length obtained by cutting both 115 and 140 cm long samples into 12.5 cm segments and carrying out the combined NIR–FIR spectral response analysis. Such analysis yielded a thickness variation of 0.5 μm ± 39% and 0.7 μm ± 57%, for 10–11 μm and 15–16 μm PS thin films, respectively. Such dielectric thin film variation is low enough to be considered negligible for all but those applications requiring the lowest loss. The extensive spectral characterization of Ag/PS HGW samples fabricated via this improved DLPD methodology demonstrated that this fabrication method is indeed successful for the fabrication of next-generation Ag/PS HGWs exhibiting low loss in the FIR (terahertz) region.

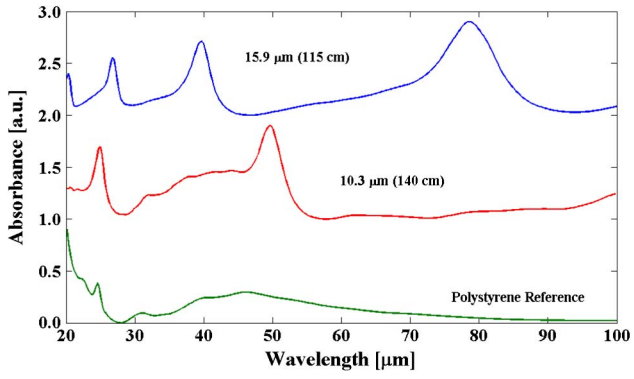

Fig. 8. Experimental FIR spectral responses of Ag/PS HWs having dielectric PS film thicknesses of 10.3 μm PS (140 cm) and 15.9 μm (120 cm) 10.3 μm along with the PS thin-film reference spectrum.

5. Conclusion

The present study describes the successful fabrication of low-loss THz HWs involving an enhanced reflective coating of an optical thin film consisting of PS on a reflective silver surface. Through the controlled DLPD of a PS thin film from aqueous PS solutions using an open vacuum-pump system, high-quality polystyrene thin films have been deposited on silver-coated hollow-glass waveguides. In comparison to prior polymer-coated HWs, the PS-coated HGWs present highly improved PS dielectric thin films capable of low-loss delivery of THz radiation. Through spectroscopic analysis from $\lambda = 1$–100 μm, PS-coated HGWs having high-quality PS thin films ranging from approximately 10–16 μm fabricated using the improved DLPD fabrication methodology presented in this study have been extensively qualitatively and quantitatively analyzed. The experimental near- to far-IR spectral response for the samples has been thoroughly examined and compared to both the theoretically expected and pure polystyrene responses. Sharp interference fringes of alternating high (*s*-polarized) and low (*p*-polarized) intensities can be seen throughout the IR spectral region and have been used for qualitative and quantitative analysis of deposited PS films. Using a 15 wt. % PS solution concentration, average PS thin film thicknesses was found to be dependent on the total waveguide length using a fixed volume of PS coating material yielded mean PS film thicknesses of 10.25 μm ± 10% and 15.9 μm ± 14%, for the 140 and 115 cm long samples, respectively. The PS film thickness was seen to vary minimally along the waveguide length regardless of total sample length and can, for nearly all practical purposes, be considered constant. The fabricated Ag/PS HGWs have been successfully optimized for low-loss transmission of THz radiation ranging from $\nu \approx 2.36$–3.66 THz depending on PS film thickness or, equivalently, total sample length. The Ag/PS HGWs fabricated in this study provide attractive low-loss THz waveguides having PS thin film thickness-dependent, tunable optical response.

The authors would like to thank the Bruker Corporation, Billerica, Massachusetts, for its contribution in measuring the spectral response of fabricated samples in the FIR region. Additionally, the authors would like to extend their gratitude to Dr. Oleg Mitrofanov of Imperial College of London, London, United Kingdom, and Dr. Miriam Vitiello of the Consiglio Nazionale delle Ricerche, University of Bari, Bari, Italy.

References

1. G. Gallot, S. P. Jamison, R. W. McGowan, and D. Grischkowsky, "Terahertz waveguides," J. Opt. Soc. Am. B **17**, 851–863 (2000).

2. D. Mittleman, *Sensing with Terahertz Radiation* (Springer, 2003).
3. K. Wang and D. M. Mittleman, "Metal wires for terahertz wave guiding," Nature **432**, 376–379 (2004).
4. H. Pahlevaninezhad, B. Heshmat, and T. E. Darcie, "Advances in terahertz waveguides and sources," IEEE Photon. J. **3**, 307–310 (2011).
5. B. Bowden, J. A. Harrington, and O. Mitrofanov, "Silver/polystyrene-coated hollow glass waveguides for the transmission of terahertz radiation," Opt. Lett. **32**, 2945–2947 (2007).
6. B. Bowden, J. A. Harrington, and O. Mitrofanov, "Low-loss modes in hollow metallic terahertz waveguides with dielectric coatings," Appl. Phys. Lett. **93**, 181104 (2008).
7. C. M. Bledt and J. A. Harrington, "Silver and silver/polystyrene coated hollow glass waveguides for the transmission of infrared radiation," Proc. SPIE **8218**, 821809 (2012).
8. U. Siciliani de Cumis, J.-H. Xu, C. M. Bledt, J. A. Harrington, A. Tredicucci, and M. S. Vitiello, "Flexible, low-loss waveguide designs for efficient coupling to quantum cascade lasers in the far-infrared," J. Infrared Millim. Terahertz Waves **33**, 319–326 (2012).
9. M. S. Vitiello, J. H. Xu, F. Beltram, A. Tredicucci, O. Mitrofanov, J. A. Harrington, H. E. Beere, and D. A. Ritchie, "Guiding a terahertz quantum cascade laser into a flexible silver-coated waveguide," J. Appl. Phys. **110**, 063112 (2011).
10. O. Mitrofanov, R. James, F. A. Fernandez, T. K. Mavrogordatos, and J. A. Harrington, "Reducing transmission losses in hollow THz waveguides," IEEE Trans. Terahertz Sci. Technol. **1**, 124–132 (2011).
11. J. A. Harrington, *Infrared Fiber Optics and Their Applications* (SPIE, 2004).
12. M. Miyagi and S. Kawakami, "Design theory of dielectric-coated circular metallic waveguides for infrared transmission," J. Lightwave Technol. **2**, 116–126 (1984).
13. P. D. Cunningham, N. N. Valdes, F. A. Vallejo, L. M. Hayden, B. Polishak, X.-H. Zhou, J. Luo, A. K.-Y. Jen, J. C. Williams, and R. J. Twieg, "Broadband terahertz characterization of the refractive index and absorption of some important polymeric and organic electro-optic materials," J. Appl. Phys. **109**, 043505 (2011).
14. M. A. Ordal, L. L. Long, R. J. Bell, S. E. Bell, R. R. Bell, R. W. Alexander, Jr., and C. A. Ward, "Optical properties of the metals Al, Co, Cu, Au, Fe, Pb, Ni, Pd, Pt, Ag, Ti, and W in the infrared and far infrared," Appl. Opt. **22**, 1099–1119 (1983).
15. C. M. Bledt, J. A. Harrington, and J. M. Kriesel, "Loss and modal properties of Ag/AgI hollow glass waveguides," Appl. Opt. **51**, 3114–3119 (2012).
16. M. Miyagi and S. Kawakami, "Waveguide loss evaluation by the ray-optics method," J. Opt. Soc. Am. **73**, 486–489 (1983).
17. Y. Matsuura, M. Saito, and M. Miyagi, "Loss characteristics of circular hollow waveguides for incoherent infrared light," J. Opt. Soc. Am. A **6**, 423–427 (1989).
18. S. J. Orfanidis, *Electromagnetic Waves and Antennas* (Rutgers University, 2010).